

Study of the $K_L^0 \rightarrow \pi^+ \pi^- \gamma$ Direct Emission Vertex

A. Alavi-Harati,¹² T. Alexopoulos,¹² M. Arenton,¹¹ K. Arisaka,² S. Averitte,¹⁰ A. R. Barker,⁵ L. Bellantoni,⁷ A. Bellavance,⁹ J. Belz,^{10,*} R. Ben-David,⁷ D. R. Bergman,¹⁰ E. Blucher,⁴ G. J. Bock,⁷ C. Bown,⁴ S. Bright,⁴ E. Cheu,¹ S. Childress,⁷ R. Coleman,⁷ M. D. Corcoran,⁹ G. Corti,¹¹ B. Cox,¹¹ M. B. Crisler,⁷ A. R. Erwin,¹² R. Ford,⁷ A. Glazov,⁴ A. Golossanov,¹¹ G. Graham,⁴ J. Graham,⁴ K. Hagan,¹¹ E. Halkiadakis,¹⁰ J. Hamm,¹ K. Hanagaki,⁸ S. Hidaka,⁸ Y. B. Hsiung,⁷ V. Jejer,¹¹ D. A. Jensen,⁷ R. Kessler,⁴ H. G. E. Kobrak,³ J. LaDue,⁵ A. Lath,¹⁰ A. Ledovskoy,¹¹ P. L. McBride,⁷ P. Mikelsons,⁵ E. Monnier,⁴ T. Nakaya,⁷ K. S. Nelson,¹¹ H. Nguyen,⁷ V. O'Dell,⁷ M. Pang,⁷ R. Pordes,⁷ V. Prasad,⁴ B. Quinn,⁴ E. J. Ramberg,⁷ R. E. Ray,⁷ A. Roodman,⁴ M. Sadamoto,⁸ S. Schnetzer,¹⁰ K. Senyo,⁸ P. Shanahan,⁷ P. S. Shawhan,⁴ J. Shields,¹¹ W. Slater,² N. Solomey,⁴ S. V. Somalwar,¹⁰ R. L. Stone,¹⁰ I. Suzuki,⁸ E. C. Swallow,^{4,6} S. A. Taegar,¹ R. J. Tesarek,¹⁰ G. B. Thomson,¹⁰ P. A. Toale,⁵ A. Tripathi,² R. Tschirhart,⁷ S. E. Turner,² Y. W. Wah,⁴ J. Wang,¹ H. B. White,⁷ J. Whitmore,⁷ B. Winstein,⁴ R. Winston,⁴ T. Yamanaka,⁸ and E. D. Zimmerman⁴

(KTeV Collaboration)

¹University of Arizona, Tucson, Arizona 85721

²University of California at Los Angeles, Los Angeles, California 90095

³University of California at San Diego, La Jolla, California 92093

⁴The Enrico Fermi Institute, The University of Chicago, Chicago, Illinois 60637

⁵University of Colorado, Boulder, Colorado 80309

⁶Elmhurst College, Elmhurst, Illinois 60126

⁷Fermi National Accelerator Laboratory, Batavia, Illinois 60510

⁸Osaka University, Toyonaka, Osaka 560 Japan

⁹Rice University, Houston, Texas 77005

¹⁰Rutgers University, Piscataway, New Jersey 08855

¹¹The University of Virginia, Charlottesville, Virginia 22901

¹²University of Wisconsin, Madison, Wisconsin 53706

(Received 25 August 2000)

We have performed studies of the $K_L^0 \rightarrow \pi^+ \pi^- \gamma$ direct emission (DE) and inner Bremsstrahlung (IB) vertices, based on data collected by KTeV during the 1996 Fermilab fixed target run. We find $a_1/a_2 = -0.737 \pm 0.034 \text{ GeV}^2$ for the DE form-factor parameter in the ρ -propagator parametrization, and report on fits of the form factor to linear and quadratic functions as well. We concurrently measure $\Gamma(K_L^0 \rightarrow \pi^+ \pi^- \gamma, E_\gamma^* > 20 \text{ MeV})/\Gamma(K_L^0 \rightarrow \pi^+ \pi^-) = (20.8 \pm 0.3) \times 10^{-3}$, and a $K_L^0 \rightarrow \pi^+ \pi^- \gamma$ DE/(DE + IB) branching ratio of 0.683 ± 0.011 .

DOI: 10.1103/PhysRevLett.86.761

PACS numbers: 13.25.Es, 11.30.Er, 12.39.Fe, 13.40.Hq

The decay $K_L^0 \rightarrow \pi^+ \pi^- \gamma$ (Fig. 1) is a potential new window into the phenomenon of CP violation [1–3]. This decay arises primarily from the CP -violating electric dipole ($E1$) “inner Bremsstrahlung” (IB) and the CP -conserving magnetic dipole ($M1$) “direct emission” (DE) processes. KTeV recently reported [4] the observation of a CP -violating angular asymmetry between the $\pi^+ \pi^-$ and $e^+ e^-$ decay planes in the $K_L^0 \rightarrow \pi^+ \pi^- \gamma^*$, $\gamma^* \rightarrow e^+ e^-$ mode, arising from the interference of DE and IB photon polarization states [5–7]. If an $E1$ DE term were also present, this could generate a direct CP -violating effect.

Understanding the precise photon energy (E_γ^*) spectrum from the DE amplitude is crucial to interpretation of CP -violating effects and may shed light on particular chiral models [8]. Previous experiments [9,10] have observed evidence for an energy shift in the DE E_γ^* spectrum, interpreted as evidence for an E_γ^* -dependent form-factor modification to the pure- $M1$ DE amplitude. Here we report on

the first measurement of this form factor from direct fits to the data, using the rare decay mode $K_L^0 \rightarrow \pi^+ \pi^- \gamma$.

We consider two separate form-factor parametrizations. Historically, the ρ -propagator form [8]

$$\mathcal{F} = \frac{a_1}{(m_\rho^2 - m_K^2) + 2m_K E_\gamma^*} + a_2 \quad (1)$$

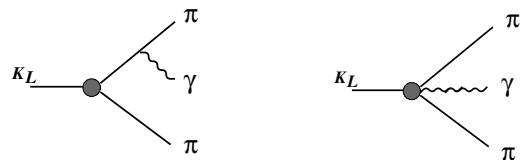


FIG. 1. The decay $K_L^0 \rightarrow \pi^+ \pi^- \gamma$ arises primarily from the contributions of the electric dipole ($E1$) “inner Bremsstrahlung” (left) and magnetic dipole ($M1$) “direct emission” (right) diagrams above.

has been used, where a_1/a_2 is the quantity of interest. More generally the form factor may be expressed as a Taylor series in E_γ^*

$$\mathcal{F} = \left(1 + \frac{rE_\gamma^*}{M_K} + \frac{sE_\gamma^{*2}}{M_K^2} + \dots \right), \quad (2)$$

where the interesting quantities are the slope r and the quadratic parameter s [11,12].

The data presented here were collected by KTeV operating in the E832 configuration [13] during the 1996 Fermilab fixed target run. A proton beam of intensity $\sim 3 \times 10^{12}$ protons per 19 sec spill incident at an angle of 4.8 mrad on a BeO target was employed to produce two nearly parallel K_L^0 beams. In E832, one of these beams was incident on an active K_S^0 regenerator. Data collected in the regenerator beam were ignored for this analysis. The E832 detector consisted of a vacuum decay region, a magnetic spectrometer with four drift chambers, photon vetoes, a

trigger scintillator bank, a CsI electromagnetic calorimeter, and a muon veto bank.

Signal $K_L^0 \rightarrow \pi^+ \pi^- \gamma$ and normalization $K_L^0 \rightarrow \pi^+ \pi^-$ candidates were selected from the two-charged-track trigger. Offline, the samples were further purified by requiring the presence of two reconstructed tracks with a good vertex χ^2 within the fiducial aperture of the detector, and no significant activity in the photon veto counters. The two-track vertex was required to be located within the vacuum (non-regenerator) beam. The tracks' kinematics were required to be inconsistent with $\Lambda^0 \rightarrow p^+ \pi^-$ decays. The energy deposited by the charged pions in the calorimeter was required to be less than $0.85 \times$ the spectrometer momentum in order to eliminate backgrounds from K_{e3} decays. Candidate events were required to have a decay vertex between 110 and 156 m downstream of the target and a total energy between 20 and 160 GeV.

$K_L^0 \rightarrow \pi^+ \pi^- \gamma$ candidates were subject to the additional criterion of requiring that the quantity

$$P_{\pi^0}^2 \equiv \frac{(M_K^2 - M_{\pi^0}^2 - M_{\pi\pi}^2)^2 - 4M_{\pi^0}^2 M_{\pi\pi}^2 - 4M_K^2 (P_T^2)_{\pi\pi}}{4[(P_T^2)_{\pi\pi} + M_{\pi\pi}^2]} \quad (3)$$

be negative, i.e., by requiring that the π^0 momentum be imaginary under a $K_L^0 \rightarrow \pi^+ \pi^- \pi^0$ hypothesis. This cut virtually eliminates the $K_L^0 \rightarrow \pi^+ \pi^- \pi^0$ background to the $K_L^0 \rightarrow \pi^+ \pi^- \gamma$ event sample. In addition, at least one non-track-associated cluster in the calorimeter was required to possess ≥ 1.5 GeV of energy, and to be at least 3 cm removed from the calorimeter edges. This "photon cluster" had to be at least 20 cm from the nearest track projection to reject background from $K_L^0 \rightarrow \pi^+ \pi^-$ events accompanied by pion hadronic showers in the calorimeter. The photon was required to have an energy of at least 20 MeV in the three-body center of momentum.

Figures 2(a) and 2(b) show the vacuum beam $K_{L,S}^0 \rightarrow \pi^+ \pi^- \gamma$ data after final cuts. A very clean signal of 8 669 $K_{L,S}^0 \rightarrow \pi^+ \pi^- \gamma$ events is achieved, with a background of about 0.5%. Approximately 0.6% of the events in the peak in Fig. 2 are residual $K_S^0 \rightarrow \pi^+ \pi^- \gamma$ decays from K_S^0 's generated at the production target. A total of 4 482 706

$K_L^0 \rightarrow \pi^+ \pi^-$ events were accumulated for the normalization sample with a 0.1% background.

To extract the direct emission form factor, we consider the distribution in E_γ^* , the photon energy in the center of momentum (Fig. 3). We wish to extract the relative contributions of the inner Bremsstrahlung and DE terms, as well

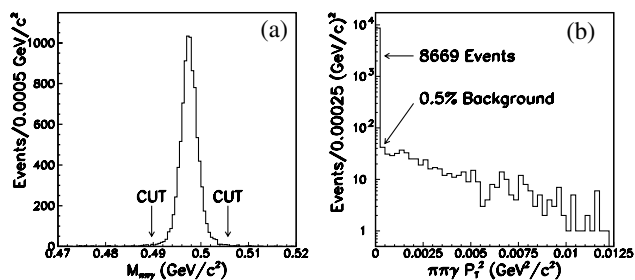


FIG. 2. (a) $M_{\pi\pi\gamma}$ distribution of candidate $K_L^0 \rightarrow \pi^+ \pi^- \gamma$ events, all other cuts applied. Arrows indicate final cuts at $M_K \pm 8 \text{ MeV}/c^2$. (b) Kaon transverse momentum squared (P_T^2) distribution of candidate $K_L^0 \rightarrow \pi^+ \pi^- \gamma$ events, all other cuts applied. The cut on this quantity requires events to be within the first bin ($0.000250 \text{ GeV}^2/c^2$) on this plot.

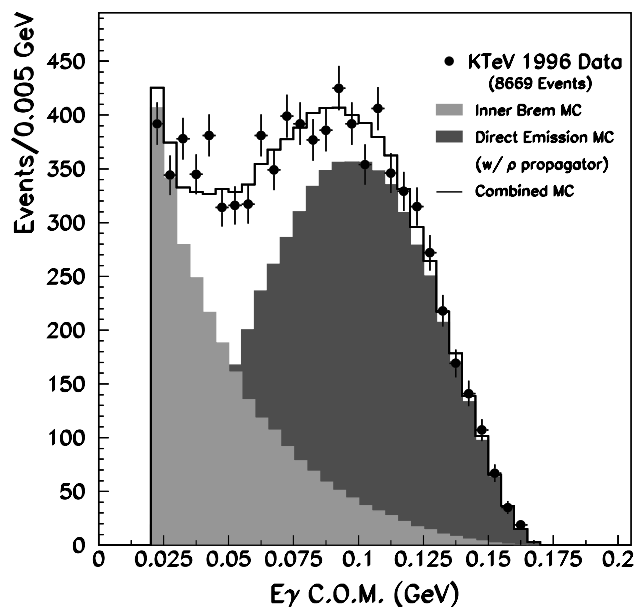


FIG. 3. $K_L^0 \rightarrow \pi^+ \pi^- \gamma$ Monte Carlo/data overlay of photon energy distribution in the center of mass, for the ρ -propagator fit result (Table I). Shown also (shaded) are the expected distributions for pure $E1$ inner Bremsstrahlung and form-factor-modified $M1$ direct emission. The "combined" Monte Carlo plot shown assumes these two are the only contributions to the decay.

as the energy shift of the DE spectrum due to the presence of a form factor. We assume that $E1$ IB and form-factor-modified $M1$ DE are the only significant contributions to the decay. We perform a MINUIT [14] χ^2 -minimization fit to combine Monte Carlo DE and IB E_γ^* distributions, and extract the relative DE and IB contributions to the data as well as the DE form factor. In the fit, the form-factor parameters (a_1/a_2 or r and s) and the ratio

$$f = \frac{\Gamma_{\text{DE}}}{(\Gamma_{\text{DE}} + \Gamma_{\text{IB}})} \quad (4)$$

are allowed to float simultaneously. A χ^2 is formed from comparison of the resultant DE + IB summed Monte Carlo histogram with the data, and minimized to obtain the best fit result.

Table I summarizes the numerical fitting results for the three form-factor parametrizations. For the Taylor series parametrization, fits were performed with the quadratic parameter both fixed at zero (floating a single parameter r_1) and allowed to vary (floating two parameters r_2 and s_2). Data Monte Carlo agreement in the E_γ^* distribution is shown in Fig. 3, for the ρ -propagator form. Figure 4 illustrates the expected effect of the various parametrizations on the pure $M1$ direct emission spectrum.

We see in the data presented in Table I and Fig. 4 clear evidence for a modification to the pure- $M1$ DE spectrum. All fits are good, though the ρ -propagator hypothesis stands out slightly: It gives the best χ^2 for a single-parameter fit, and the two-parameter fit results are in good agreement with the values $r_2 = -2.70$ and $s_2 = 3.87$ obtained by Taylor expanding the ρ -propagator form. The size of this energy shift, in particular the need to take into account terms of second order in E_γ^* , is not currently understood within the chiral perturbation theory model for this decay [11].

Additional contributions to the photon energy spectrum are expected from CP -violating higher-order multipole contributions to the direct emission amplitude. One possible consequence of these multipole terms is the presence of a charge asymmetry in the π^+ versus π^- Dalitz plot [1]. We exclude asymmetries larger than 2.4% at 90% C.L. with the present data.

One might also expect a contribution to the E_γ^* spectrum from CP -violating $E1$ DE, which could interfere with the $E1$ IB. We have allowed for such a term, by performing a separate fit in which we assumed an $E1$ DE amplitude con-

stant in E_γ^* , and searched for the corresponding interference contribution [12] to the E_γ^* spectrum. The form-factor parameter and f [see Eq. (4)] are allowed to float simultaneously, while fixing the IB rate at its theoretical value of 7.00×10^{-3} [1]. Based on this fit, we set an upper limit of $\Gamma_{\text{IN}}/(\Gamma_{\text{DE}} + \Gamma_{\text{IB}} + \Gamma_{\text{IN}}) \leq 0.30$ (90% C.L.) on the contribution to the decay rate of the CP -violating interference term. $\Gamma_{\text{IN}}/\Gamma_{\text{ALL}} = 0.30$ corresponds to a 22% decrease in the $\Gamma_{\text{DE}}/\Gamma_{\text{ALL}}$ ratio.

Background subtraction under the E_γ^* distribution (with shape determined by study of P_T^2 sideband) resulted in no statistically significant change in either the form-factor parameter or the DE/(DE + IB) ratio. Accidental activity in the detector was also found to have no statistically significant effect. The form-factor parameters are found to have a slight (1.9%) sensitivity to variations of the lower E_γ^* cutoff (nominally 20 MeV) used in the fit. We also assign systematic uncertainties of 1.8% due to detector acceptance, and 1.4% due to the effects of uncertainties in the calorimeter photon energy scale.

Note (Table I) that the measured DE/(DE + IB) ratio is insensitive to the particular choice of form-factor parametrization. Uncertainty in the detector acceptance contributes a 0.7% systematic uncertainty to this ratio, while variations in analysis cuts contribute 0.6%. The systematic uncertainty due to the calorimeter photon energy scale is 0.2%.

We find the absolute $K_L^0 \rightarrow \pi^+ \pi^- \gamma$ branching ratio by normalizing the signal to the $K_L^0 \rightarrow \pi^+ \pi^-$ channel. We determine the ratio of $K_L^0 \rightarrow \pi^+ \pi^- \gamma / K_L^0 \rightarrow \pi^+ \pi^-$ acceptances using a Monte Carlo simulation of the full detector and offline analysis criteria. Based on this, we calculate $\Gamma(K_L^0 \rightarrow \pi^+ \pi^- \gamma) / \Gamma(K_L^0 \rightarrow \pi^+ \pi^-) = (20.8 \pm 0.2 \text{ stat} \pm 0.2 \text{ syst}) \times 10^{-3}$ for $K_L^0 \rightarrow \pi^+ \pi^- \gamma$ events with $E_\gamma^* > 20$ MeV. The systematic uncertainty is due primarily to the effects of K_S^0 contamination in the vacuum beam. Assuming no contribution from interference and using the DE/(DE + IB) result from Table I, we obtain the final $\pi^+ \pi^-$ -normalized branching ratios $(14.2 \pm 0.2 \pm 0.2) \times 10^{-3}$ for direct emission and $(6.6 \pm 0.2 \pm 0.2) \times 10^{-3}$ for inner Bremsstrahlung.

Our measured IB branching ratio is consistent with both the QED prediction of 7.00×10^{-3} and the most recent experimental result of FNAL E731 [10]; $(7.3 \pm 0.4) \times 10^{-3}$, based on a sample of 3 136 $K_L^0 \rightarrow \pi^+ \pi^- \gamma$ events. The DE/(DE + IB) ratio is also in good agreement with

TABLE I. Summary of $K_L^0 \rightarrow \pi^+ \pi^- \gamma$ fit results for the three form-factor parametrizations. The first uncertainty is statistical; the second is systematic.

Quantity	ρ propagator	Linear	Quadratic
$\chi^2/\text{d.o.f.}$	38.8/27	43.2/27	37.6/26
a_1/a_2	$(-0.737 \pm 0.026 \pm 0.022) \text{ GeV}^2$
r	...	$-1.739 \pm 0.062 \pm 0.052$	$-2.93 \pm 0.41 \pm 0.34$
s	$3.31 \pm 1.15 \pm 0.96$
f	$0.683 \pm 0.009 \pm 0.007$	$0.682 \pm 0.009 \pm 0.007$	$0.684 \pm 0.011 \pm 0.007$

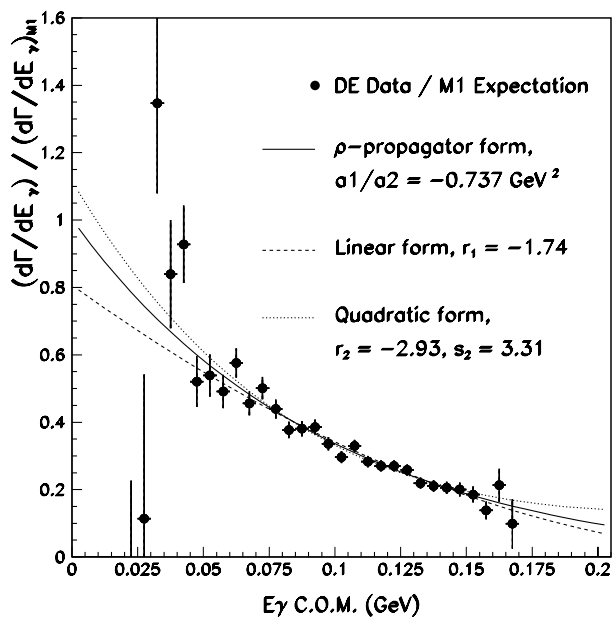


FIG. 4. Ratio (points) of (IB-subtracted) direct-emission data to the expectation for a pure $M1 E_\gamma^*$ spectrum. Vertical scale is arbitrary. Shown for comparison are the best-fit results (Table I) for the ρ -propagator (solid), linear (dashed), and quadratic (dotted) form-factor parametrizations. A modification to the pure- $M1$ spectrum is clearly supported by the data.

the E731 result of 0.685 ± 0.041 . The present form-factor results differ significantly from that reported by E731 ($a_1/a_2 = -1.8 \pm 0.2 \text{ GeV}^2$) but this discrepancy has been understood: The E731 a_1/a_2 form factor was *inferred* [15] from the model of Lin and Valencia [8], on the basis of the measured DE branching ratio, whereas our results are obtained *directly* by performing fits to the E_γ^* distribution. The underlying datasets in the two experiments are consistent with each other, and a reanalysis of the E731 data using our method yields results consistent with ours. The KTeV $K_L^0 \rightarrow \pi^+ \pi^- \gamma$ DE form-factor result is also in good agreement with the result $a_1/a_2 = -0.720 \pm 0.029 \text{ GeV}^2$ extracted from the independent $K_L^0 \rightarrow \pi^+ \pi^- e^+ e^-$ analysis from the KTeV E799 data set [4].

In conclusion, we have made the first direct measurements of the $K_L^0 \rightarrow \pi^+ \pi^- \gamma$ direct emission form factor, including $a_1/a_2 = -0.737 \pm 0.034 \text{ GeV}^2$. We find no evidence for new CP -violating effects in the photon energy spectrum. Finally, we have made improved measurements of the DE $[(14.2 \pm 0.2 \pm 0.2) \times 10^{-3}]$ and IB $[(6.6 \pm 0.2 \pm 0.2) \times 10^{-3}]$ $K_L^0 \rightarrow \pi^+ \pi^- \gamma$ branching ratios, normalized to the $K_L^0 \rightarrow \pi^+ \pi^-$ channel.

We thank German Valencia and Jusak Tandean for discussions concerning this work. We gratefully acknowledge the support of the technical staff of Fermilab and participating institutions. This work was supported in part by the U.S. DOE, NSF, and The Ministry of Education and Science of Japan.

*To whom correspondence should be addressed.

Electronic address: belz@physics.montana.edu

Permanent address: Montana State University, Bozeman, Montana 59717.

- [1] G. Costa and P.K. Kabir, Nuovo Cimento Soc. Ital. Fis. **51A**, 564 (1967).
- [2] L. Sehgal and L. Wolfenstein, Phys. Rev. **162**, 1362 (1967).
- [3] G. D'Ambrosio and G. Isidori, Int. J. Mod. Phys. **A13**, 1 (1998).
- [4] A. Alavi-Harati *et al.*, Phys. Rev. Lett. **84**, 408 (2000).
- [5] L. Sehgal and M. Wanninger, Phys. Rev. D **46**, 1035 (1992); **46**, 1035(E) (1992).
- [6] P. Heiliger and L. M. Sehgal, Phys. Rev. D **48**, 4146 (1993).
- [7] J.K. Elwood *et al.*, Phys. Rev. D **52**, 5095 (1995); J.K. Elwood *et al.*, Phys. Rev. D **53**, 2855(E) (1996); J.K. Elwood *et al.*, *ibid.* **53**, 4078 (1996).
- [8] Y. C. R. Lin and G. Valencia, Phys. Rev. D **37**, 143 (1988).
- [9] A. Carroll *et al.*, Phys. Rev. Lett. **44**, 529 (1980).
- [10] E. J. Ramberg *et al.*, Phys. Rev. Lett. **70**, 2525 (1993).
- [11] G. Ecker, H. Neufeld, and A. Pich, Nucl. Phys. **B413**, 321 (1994).
- [12] L. Littenberg and G. Valencia, Annu. Rev. Nucl. Part. Sci. **43**, 729 (1993).
- [13] A. Alavi-Harati *et al.*, Phys. Rev. Lett. **83**, 22 (1999).
- [14] F. James and M. Roos, Comput. Phys. Commun. **10**, 343 (1975).
- [15] E. Ramberg (private communication).